CERN-PPE/90-183
11 December 1990

EUROPEAN ORGANIZATION FOR NUCLEAR RESEARCH

Measurement of the Stopping Power of Silicon for Antiprotons between 0.2 and 3 MeV

R. Medenwaldt, S. P. Møller, E. Uggerhøj, and T. Worm

Institute for Synchrotron Radiation, Aarhus University
Ny Munkegade, DK-8000 Aarhus C, Denmark

P. Hvelplund and H. Knudsen

Institute of Physics, University of Aarhus
DK-8000 Aarhus C, Denmark

K. Elsener

CERN, CH-1211 Geneve 23, Switzerland

E. Morenzoni

Paul Scherrer Institute, CH-5232 Villigen PSI, Switzerland

Abstract

Our previous measurement of the stopping power of silicon for antiprotons has been extended down to 200 keV. The antiproton-stopping power is found to be more than 30 % lower than that for equivelocity protons at 200 keV. The "Z_1^3 contribution" to the stopping power (the Barkas effect) is deduced by comparing the stopping power for protons and antiprotons. Comparisons to theoretical estimates are made.

(submitted to Nucl. Instrum. Methods Phys. Res. B)

1. Introduction

Although the slowing-down of fast charged particles in matter has been studied for more than half a century, there is still a need for a better understanding of the energy-loss process. This not only bears on practical questions of predicting the slowing-down, but also fundamental questions related to the basic atomic-collision processes involved are still unresolved. With the advent of the low-energy antiproton facility LEAR at CERN, we started to use these high-quality beams of heavy negatively charged particles to study deviations from exact invariance of the stopping power under projectile charge conjugation.[1,2,3].

A difference in the stopping power for positive and negative particles (the Barkas effect) has been known for a long time[4], but lack of suitable antiparticle beams has prohibited quantitative studies of the effect. The Barkas effect can also be deduced by comparisons of the stopping power for protons, alpha particles and lithium nuclei[5], but the interpretation of these data is not as straightforward as particle/antiparticle data. Furthermore the antiparticle measurements can be performed at much lower energies than with alfa particles and lithium nuclei owing to electron capture effects. Actually, the absence of electron capture for negative particles makes their stopping powers better suited for comparisons with calculations.

2. Theory

The basic stopping-power formula in the high-energy limit is the Bethe formula[6],

$$-dE/dx = (4\pi e^2 N Z_2/mv^2) Z_1^2 L_0, \qquad (1)$$

which is derived in the first Born approximation. Hence the stopping power is proportional to the square of the projectile charge Z_1. In eq. (1), v is the projectile velocity, N the target density and Z_2 the target atomic number. The Bethe stopping function, which is independent of Z_1, may be written as

$$L_0 = \ln[2mv^2/I(1-v^2/c^2)] - v^2/c^2 - C/Z_2, \quad (2)$$

where I is the mean ionization potential and C/Z_2 the so-called shell corrections.

A Z_1^3 (Barkas) correction to the Bethe formula was first calculated by Ashley, Ritchie and Brandt[7] and by Jackson and McCarthy[8] for the distant collisions only. The effect is related to the polarization of the medium induced by the projectile. This explains qualitatively why negatively charged particles have a lower stopping power than positive ones. The authors of Refs. 7 and 8 assert, that the close collisions are essentially those of free particles, giving an exact Z_1^2 dependence. The arguments for the choice of the dividing impact parameter between close and distant collisions are, however, not obvious, in particular because the resulting stopping power depends strongly on this parameter.

Formally, one may generalize the Bethe equation to include the higher-order Z_1 terms in the stopping function,

$$L = L_0 + Z_1L_1 + Z_1^2L_2 + \ldots, \quad (3)$$

where L_1 and L_2 are the Z_1-independent coefficients of the Z_1^3 and Z_1^4 terms in the stopping power and where higher-order terms usually are omitted.

The Jackson and McCarthy result is to better than 3% given by[9]

$$L_1 = L_0[0.477 - 0.1385\ln(V + 2)]/V^2Z_2^{1/2} \quad (3)$$

for $1<V<10$ where $V=v/(Z_2^{1/2}v_0)$ and v_0 is the Bohr velocity.

Historically, the next major step was Lindhards argumentation[10], that the close collisions also contribute significantly to the Barkas effect. These collisions are *not* exactly Coulomb-like owing to dynamical screening of the projectile charge by the atomic electrons, and the close-collision contribution was estimated to be comparable to the distant-collision contribution

given by Jackson and McCarthy. Furthermore, it was shown, that the Z_1^4 correction, which includes the so-called Bloch term, is not negligible. The Bloch term is obtained as the difference between the Bethe result and Bloch's calculation of the stopping power[11], and can be given as

$$L_{2,\mathrm{Bloch}} = -1.2(\kappa_B/2)^2 \quad \text{for} \quad \kappa_B = 2|Z_1|Z_2(v/v_0) < 1. \tag{4}$$

A quantum-mechanical calculation of the stopping power for the harmonic oscillator accurate up to third order in Z_1 appeared recently[12], showing that there are significant contributions to the Z_1^3 effect for *all* impact parameters. Furthermore this model does not assume the projectile speed to be large compared to the speed of the target electrons. It is the breakdown of this assumption that gives rise to the shell corrections to the first-order Born approximation, eq. (2). Hence in this model the shell corrections are included in the calculation of the Barkas term. So within the harmonic-oscillator model, the Barkas effect can be calculated without approximations; however, two questions are still open: in what detail can atoms be represented by harmonic oscillators and does the expansion in powers of Z_1 make sense as a converging perturbation series[13].

Another widely used representation of the stopping medium is the electron gas, which is much used in the velocity-proportional stopping region below the proton stopping-power maximum. Recently, Sørensen[14] calculated the stopping power for protons and antiprotons in a classical electron gas in this velocity region. For silicon, the antiproton-stopping power is found to be around 40 % of the proton value. A quantal calculation for the static electron gas valid in the MeV region above the electronic stopping-power maximum also appeared recently[15].

For recent reviews of the experimental and theoretical situation, see Refs. 9, 16 and 17.

3. Experimental Method

Stopping powers can be obtained in several more or less direct

ways. The method used should, however, be tailored to the experimental conditions. In the present case it is the antiproton beam which sets the scene. The beam delievered by the LEAR facility, has an intensity up to a few 10^5/sec at the lowest energy of 5.91 MeV. The beam has at its focus a size of a few mm^2 and a divergence of some mrads. To obtain lower energies, the beam has to be degraded, resulting in a large divergence. Furthermore, energy straggling is introduced in the degrader, and below approximately 1 MeV, the energy spread is so large that the beam can not be considered as monoenergetic. Given these circumstances, we chose to use calorimetry for the measurements, namely by inferring the energy loss from the energy deposited in the target foil (see however Ref. 3). A very accurate calorimetric method was developed by Andersen[5,18], but this method is not well suited for an antiproton beam. Instead we have used active silicon foils, and deduced the deposited energy from the number of formed electron-hole pairs. It is then required, that the energy spent to produce an electron-hole pair, w, is projectile- and energy-independent. It is known that w is slightly lower for alfa particles than for equivelocity protons, and this difference can be ascribed to the difference in the stopping power[19]. Using the model of Ref. 19, the difference in w between antiprotons and protons in the relevant velocity range is predicted to be less than one percent.

In our previous investigations[1,2] the antiproton-stopping power was measured between 0.538 and 3.01 MeV. The measurements were limited on the low-energy side by the finite thickness of the silicon detectors used (2.9 and 5.9 μm) and by the energy-straggling of the degraded beam. We have circumvented these restrictions by using a 1.2-μm detector and by the measurement of the energy of the individual antiprotons.

The beam exits the LEAR vacuum system through a beryllium window approximately 100 μm thick and enters the experimental-vacuum chamber through a 20-μm mylar foil as shown in fig. 1. Here the beam is degraded to lower energies by aluminium foils. Since the total projectile energy is required, we measure the Time-Of-Flight (TOF) of the particles from the 100-μm thick start

scintillator to the 1-mm thick stop scintillator. The silicon detector is situated close to the start scintillator, and hence it is the exit energy which is measured by the TOF system. The TOF and energy-loss signal are accumulated on an event-by-event basis using a CAMAC system connected to a PC. The obtained time resolution is 2.7 ns (FWHM) corresponding to an energy resolution of 27 keV (FWHM) at 500 keV in our geometry. The TOF system is calibrated by standard delays and by varying the length of the flight path. The efficiency of the system is rather low at the lowest energies owing to the large multiple scattering and the small size of the silicon detector (10 mm^2). The data for the different detectors were intercalibrated by alfa sources. The resolution of the 1.2-μm detector and associated electronics is around 25 keV (FWHM) and is larger than the straggling in the detector. The stopping power is determined as $dE/dx = \Delta E/\Delta x$ at the energy $E_2 + \Delta E/2$, where E_2 is the exit energy measured by the TOF system and ΔE is the energy deposited in the detector.

4. Results

In the present experiment the antiproton stopping power was measured at two "mono-energetic" energies with the 1.2-μm detector, namely 1.28 (0.36 MeV FWHM) and 0.78 MeV (0.43 MeV FWHM). The other beam energies were obtained from an analysis of one run with a thick degrader using the TOF information. In fig.2 the distributions of deposited energies for the two energies 1.28 and 0.213 MeV are shown. The spectra are well separated from the noise and demonstrate the change in the energy loss over the energy region covered.

In fig. 3 are shown the measured antiproton-stopping powers for the three different silicon detectors. The results from the two thicker detectors[1,2] were calibrated by comparing proton measurements to the recommended values by Andersen and Ziegler[20]. The data from the thinnest detector were calibrated to these results with an alpha source and using the nominal thickness. It is seen that results from different silicon foils agree in the overlap regions. An uncertainty of 1 percent was attributed to

the measurements with the two thick detectors, and the uncertainty in the thin-foil measurements is probably somewhat larger. The full-drawn curve is the Andersen-Ziegler fit to old proton stopping powers[20], and the points are recent accurate proton stopping power measurements[21]. The measured antiproton-stopping power merge with the proton results at high energy as expected. For decreasing energy, the antiproton stopping power increases much slower than the one for protons, and at the lowest energy of 0.188 MeV, the antiproton stopping power is 32 % lower than for equivelocity protons.

In fig. 4 we have extracted the Barkas term L_1 from the data as one-half of the difference between proton stopping powers and the measured antiproton stopping power divided by the Bethe front factor, eq. (1). The proton stopping powers used above 0.7 MeV are from ref. 20 and below 0.7 MeV from ref. 21. The abscissa on fig. 4 is the velocity in units of the Bohr velocity, v_0. The full-drawn and dashed curves are the Jackson and McCarthy calculation and twice this result, respectively. For high velocities (>6 v_0), the measured Barkas term is seen to be about a factor of two larger than that calculated by Jackson and McCarthy for the distant collisions only, and in good agreement with the estimate of the Barkas term by Lindhard with equal contributions from close and distant collisions. At the lower energies, the measured Barkas term is clearly not well described by the result from this simple model. Hence, we have also plotted the Z_1^3 term from more elaborate models[13,15,22]: The dotted curve is the harmonic oscillator calculation using only one oscillator with oscillation energy corresponding to the mean ionization potential of silicon, I = 165 eV. This model fails to describe the behavior of the measured Z_1^3 term, especially at the low velocities. The dot and long-dashed curve is a static electron gas calculations with a plasma frequency of 165 eV and the dot and short-dashed curve is an electron gas calculation in the local density approximation (LDA). The constant density electron-gas result is much too large at low velocities, whereas the LDA model seems to reproduce the velocity dependence, although the result is slightly too low over the whole velocity region.

5. Comparison with other measurements

Previous measurements of the Barkas effect stem from secondary particle/antiparticle beams[4,23,24,25,26] and from ion beams[5]. Due to the low intensity and poor quality of the particle/antiparticle beams used, the obtained accuracy in these measurements is low. Using a calorimetric technique, Andersen et al.[5] measured the stopping power of fast protons, alpha particles and lithium nuclei in Al, Cu, Ag and Au targets. They derived values of L_1 which, like the ones obtained here above $5v_0$, are approximately a factor of two larger than calculated by Jackson and McCarthy[8].

6. Conclusions

We have measured antiproton stopping powers of silicon in the energy range from 0.188 to 3 MeV. The results have been compared to proton stopping powers, and the Z_1^3 correction to the Bethe-stopping power, the Barkas term, has been extracted from the data and compared to harmonic-oscillator and electron-gas calculations. Only the elaborate electron-gas calculation performed in the local-density approximation describe the measurements reasonably well over the entire velocity range ($3\text{-}11v_0$).

Extraction of physical quantities like the mean ionization potential, I, from measured proton stopping powers (see e.g. the recent ref. 27) requires knowledge about the Z_1^3 and Z_1^4 corrections to the Bethe formula, and different choices for the corrections has been made. The present series of experiments provide for the first time an accurate measurement of the Barkas correction to use in such work.

The experiment exploits the possibilities of thin transmission surface-barrier silicon detectors. With the presently available detectors (down to 1.2 μm thin) a continuation of the experiment to lower beam energies can not be envisaged. However, a new TOF technique has recently been tested successfully[3]: in addition to scintillator start and stop signals, the secondary electrons emitted upon passage of an antiproton through a thin

foil are used to provide a timing signal. With this method, antiproton stopping powers in a broad variety of materials can be measured down to energies below the 200 keV achieved in the present work.

References

[1]L. H. Andersen, P. Hvelplund, H. Knudsen, S. P. Møller, J. O. P. Pedersen, E. Uggerhøj, K. ELsener, and E. Morenzoni, Phys. Rev. Lett. **62**, 1731 (1989).

[2]S. P. Møller, Nucl. Instrum. Methods B **48**, 1 (1990).

[3]R. Medenwaldt, S. P. Møller, E. Uggerhøj, T. Worm, P. Hvelplund, H. Knudsen, K. Elsener, and E. Morenzoni, submitted to phys. lett. A.

[4]W. H. Barkas, W. Birnbaum, and F. M. Smith, Phys. Rev. **101**, 778 (1956).

[5]H. H. Andersen, J. F. Bak, H. Knudsen, and B. R. Nielsen, Phys. Rev. A **16**, 1929 (1977).

[6]H. A. Bethe, Ann. Phys. (Leipzig) **5**, 325 (1930); U. Fano, Ann. Rev. Nucl. Sci. **13**,1 (1963).

[7]J. C. Ashley, R. H. Ritchie, and W. Brandt, Phys. Rev. B **5**, 2393 (1972); Phys. Rev. A **8**, 2402 (1973).

[8]J. D. Jackson and R. L. McCarthy, Phys. Rev. B **6**, 4131 (1972).

[9]H. Bichsel, Phys. Rev. A **41**, 3642 (1990).

[10]J. Lindhard, Nucl. Instrum. Methods **132**, 1 (1976).

[11]F. Bloch, Ann. Phys. (Leipzig) **16**, 285 (1933).

[12]H. H. Mikkelsen and P. Sigmund, Phys. Rev. A **40**, 101 (1989).

[13]H. H. Mikkelsen and E. H. Mortensen, Nucl. Instrum. Methods B **48**, 39 (1990).

[14]A. H. Sørensen, Nucl. Instrum. Methods B **48**, 10 (1989).

[15]H. Esbensen and P. Sigmund, Ann. Phys. **201**, 152 (1990).

[16]G. Basbas, Nucl. Instrum. Methods B **4**, 227 (1984).

[17]H. H. Andersen, in *Semiclassical Descriptions of Atomic and Nuclear Collisions*, edited by J. Bang et al. (Elsevier, New York, 1985), p. 409.

[18]H. H. Andersen, Risø Report no. 93 (1965).

[19]W. N. Lennard, H. Geissel, K. B. Winterbon, D. Phillips, T. K. Alexander, and J. S. Forster, Nucl. Instrum. Methods A **248**, 454 (1986).

[20]H. H. Andersen and J. F. Ziegler, *Hydrogen Stopping Powers and Ranges in All Elements* (Pergamon, New York, 1977).

[21]P. Mertens and P. Bauer, Nucl. Instrum. Methods B **33**, 133

(1988).

[22]H. H. Mikkelsen, H. Esbensen and P. Sigmund, Nucl. Instrum. Methods B **48**, 8 (1990).

[23]W. H. Barkas, N. J. Dyer, and H. H. Heckman, Phys. Rev. Lett. **11**, 26 (1963).

[24]H. H. Heckman and P. J. Lindstrom, Phys. Rev. Lett. **22**, 871 (1969).

[25]W. Wilhelm, H. Daniel, and F. J. Hartmann, Phys. Lett. B **98**, 33 (1981).

[26]F. Kottmann, Proc. II Int. Symp. on Muon and Pion Interactions with matter (Dubna, 1987) p. 268.

[27]N. Shiomi-Tsuda, N. Sakamoto, H. Ogawa, and R. Ishiwari, Nucl. Instrum. Methods B **48** (1990) 61.

Figure Captions

Fig. 1 Schematic drawing of the experimental setup. The numbers refer to: 1 Beamline vacuum chamber; 2 Start scintillator; 3 Silicon detector foil and 4 Stop scintillator.

Fig. 2 Distributions of deposited energies in the 1.2-μm silicon detector for incident beam energies of 0.213 and 1.26 MeV.

Fig. 3 Measured antiproton-stopping powers compared to proton values (full-drawn line and filled symbols).

Fig. 4 The Z_1^3 contribution, L_1, to the stopping power extracted from the measurements. The curves are described in the text.

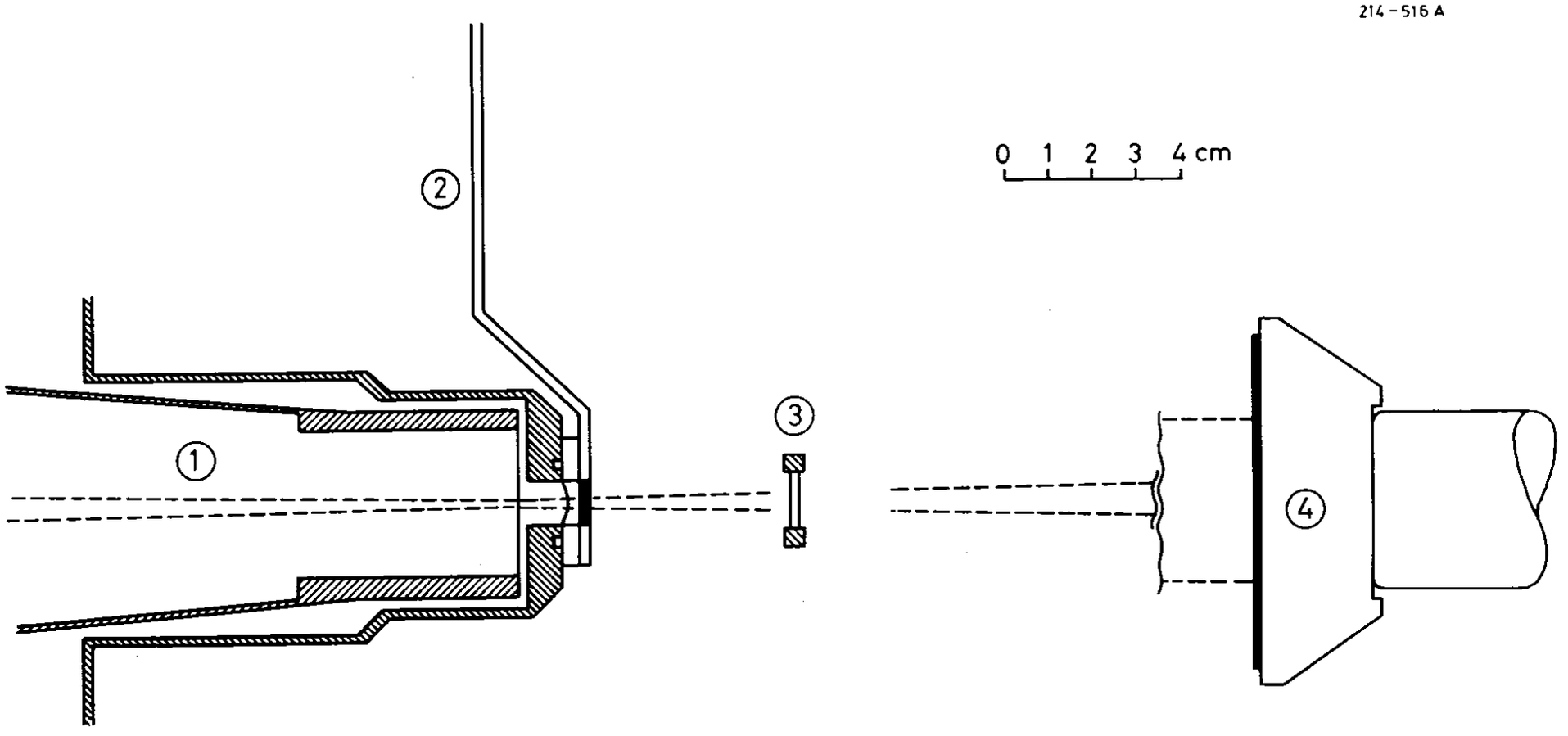

Fig. 1

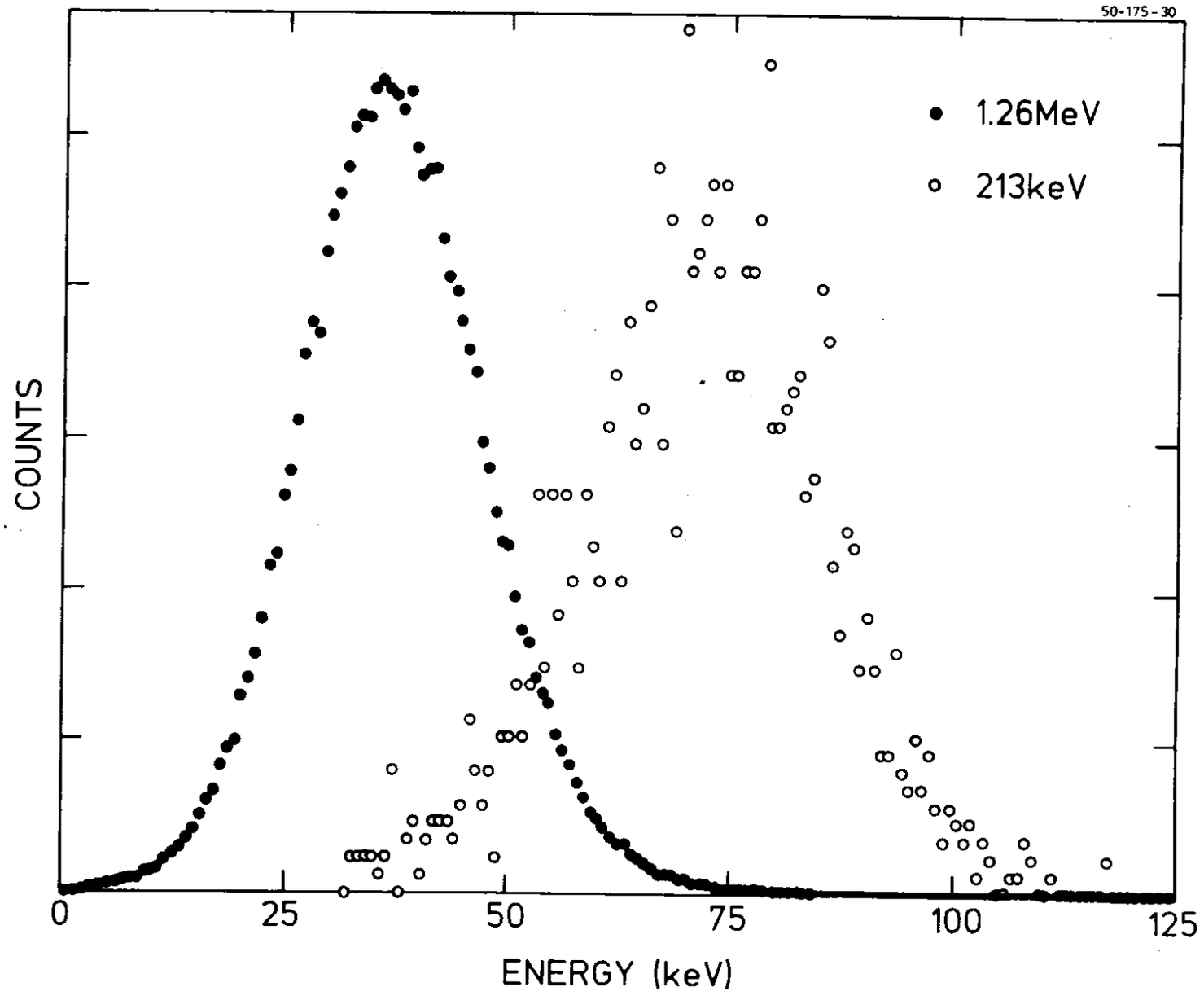

Fig. 2

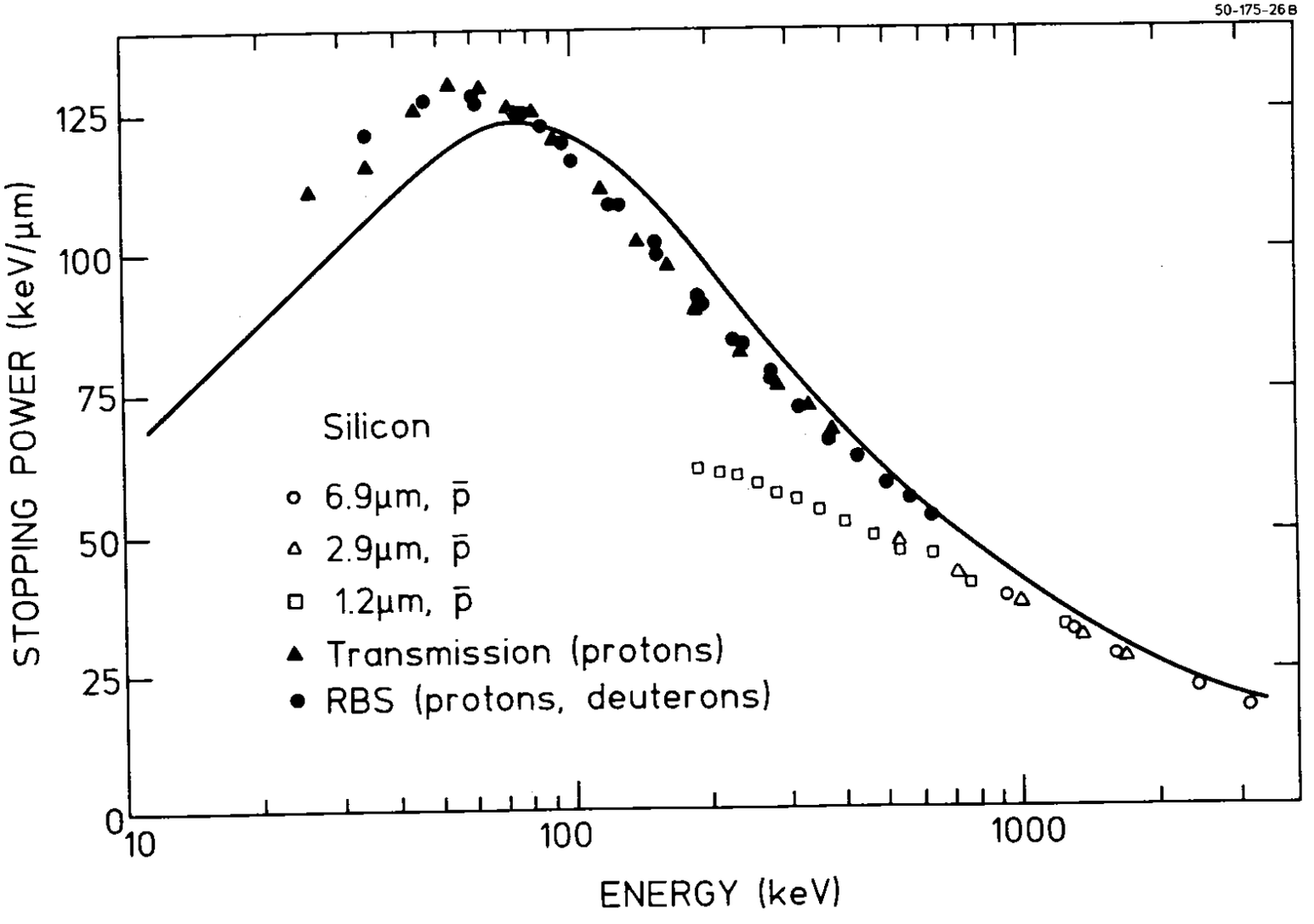
50-175-26B
STOPPING POWER (keV/μm)
125
100
75
50
25
0
10
100
1000
ENERGY (keV)
Silicon
6.9μm, p̄
2.9μm, p̄
1.2μm, p̄
Transmission (protons)
RBS (protons, deuterons)

Fig. 3

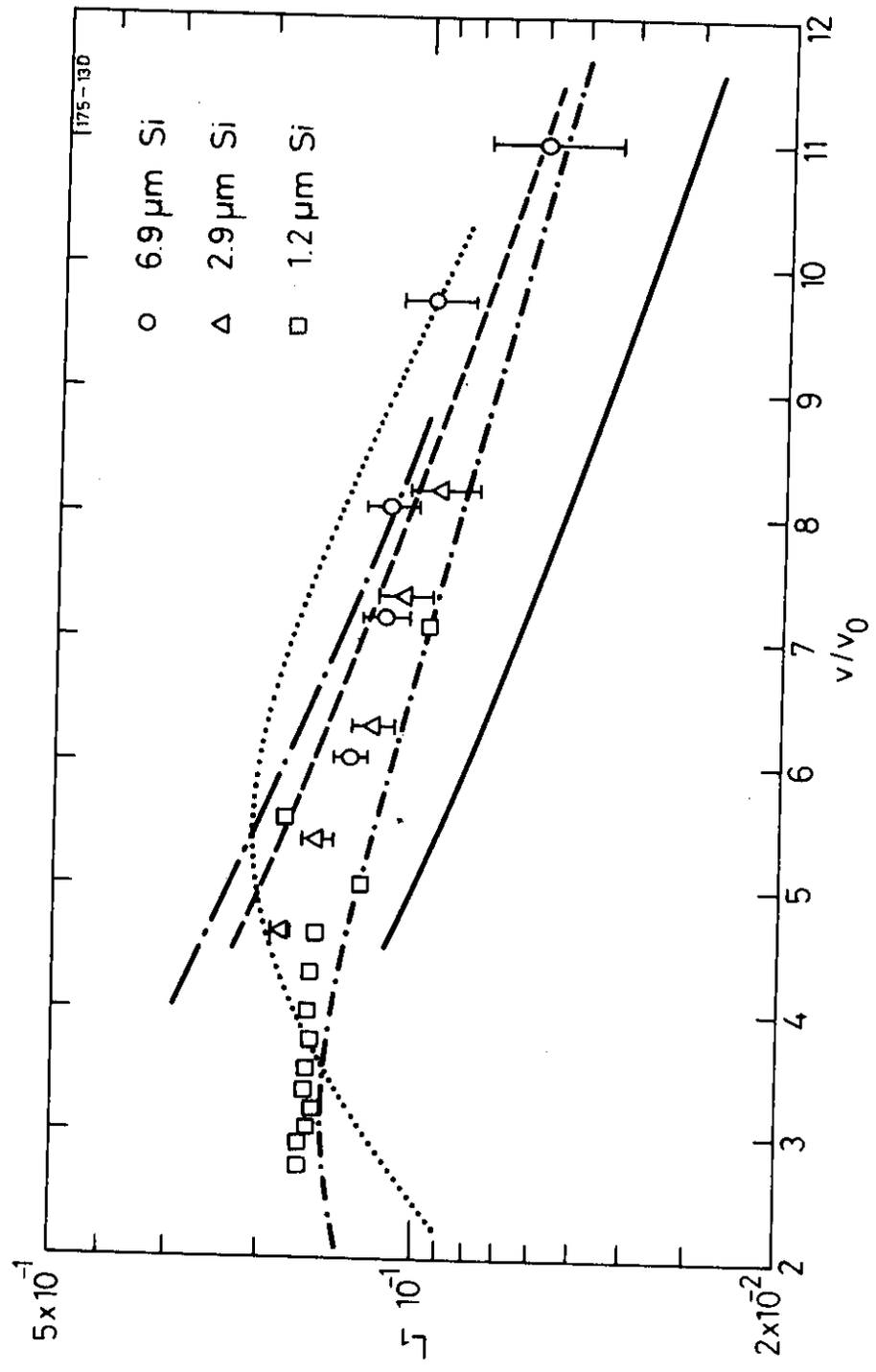

Fig. 4

Imprimé au CERN. Prix : 0.50 Fr.